Geofluids (2002) **2**, 217–232

Three-dimensional geometry, ore distribution and time-integrated mass transfer through the quartz–tourmaline–gold vein network of the Sigma deposit (Abitibi belt, Canada)

P. GAROFALO, S. K. MATTHÄI* AND C. A. HEINRICH

Eidgenössische Technische Hochschule (ETH) Zurich, Department of Earth Science, Isotope Geology and Mineral Resources, Zurich, Switzerland

ABSTRACT

We present a reconstruction of the three-dimensional (3D) geometry and gold grade distribution of shear zone-hosted, Au-mineralized, quartz–tourmaline veins of the Sigma deposit (Abitibi belt). Host shears and veins form a network of anastomosing, steeply dipping structures associated with smaller subhorizontal extensional veins. Our reconstruction has been carried out using the exceptionally large geological database of the mine. From this database, we extracted the geometric position, thickness and gold grades of geometrically best-defined steep veins contained in a representative subvolume of the deposit. These data allowed the 3D representation of 53 veins, which have been constructed by fitting surfaces through the geometrical data and by contouring thickness and gold grade. The geometry of the network is mainly characterized by: (i) a few large segmented veins, with sinuous and helicoidal shape, and typical vertical dimension of >100 m; (ii) a large number of smaller vertical veins, some of which splay off the steep veins with high dip angles; (iii) subhorizontal extension veins (joints) located at, or close to, the tips of steep veins. The absolute thickness of the vertically short veins is the same as that of the large veins, suggesting that they formed simultaneously, but only a few of them interconnect to form vertically continuous bodies. Patchy, vertically elongated zones of high dilation are present in the large veins, and are poorly correlated with Au-rich zones. They presumably represent former high-permeability zones of the network. The highest gold grades occur at the interconnections between the large veins and small splays or subhorizontal joints. This indicates the important role of vein interconnection for fluid flow and gold precipitation within the network. Combining the calculation of the volume of the network with the estimation of tourmaline abundance in the veins, we calculate that 2.1×10^6 m^3 of tourmaline and 3.2×10^6 m^3 of quartz precipitated during Au deposition.

Key words: 3D vein networks, Au deposits, tourmaline

Received 3 November 2001; accepted 11 April 2002

Corresponding author: Present address: Paolo Garofalo, Institut für Geowissenschaften, Abteilung Mineralogie und Petrologie, Peter Tunner Strasse 5, A-8700 Leoben, Austria.
E-mail: garofalo@unileoben.ac.at. Tel: +43 3842 402 453. Fax: +43 3842 47016.

Geofluids (2002) **2**, 217–232

INTRODUCTION

Vein networks have long been recognized as former channelways for fluid flow in the upper crust. Vein orientation, shape, spacing, interconnection and permeability within a network control fluid flow (Jing & Stephansson 1997), and studies on vein-hosted deposits (e.g. Ridley & Mengler 2000; Vearncombe 1998) and metamorphic hydrothermal systems (e.g. Oliver & Bons 2001) indicate that a knowledge of these parameters is essential to understand mineral precipitation in veins. Field, analogue and numerical studies on the formation of mineralized fracture networks in various geological environments (Cooke & Pollard 1996; Fisher *et al.* 1995; Martel & Pollard 1989; Nicholson & Pollard 1985; Simpson 2000; Willemse *et al.* 1996) and on the effects of changes of fault permeability on fluid flow (Matthäi & Fischer 1994; Matthäi & Roberts 1997) further confirm that these parameters exert

*Present address: Department of Earth Sciences and Engineering, Imperial College, Royal School of Mines, London, UK

important constraints on fluid flow models. Hence, investigations on fluid flow within vein networks should take into account the three-dimensional (3D) geometrical properties and the interconnection (i.e. topology in the sense of Jing & Stephansson 1997) of network veins.

Many studies of natural vein systems lack a knowledge of the 3D network geometry because of limitations in exposure. In contrast, underground mining offers an opportunity to directly access and record geometrical data on natural vein networks in three dimensions. Such data comprise a wealth of geometrical information stored in level plans, borehole logs and vertical sections, which are compiled over kilometre-scale intervals and can be used for the reconstruction of network geometry. Moreover, data on ore distribution within these networks directly elucidate the relationships between the ore grade and geometrical characteristics of veins, and can therefore be used to gain insights into the mechanisms of ore precipitation.

In this study, we present a reconstruction of the 3D geometry and gold grade distribution of 53 steeply dipping veins excavated from an 800-m vertical interval in the quartz–tourmaline vein network of the Sigma deposit (Quebec). Due to the large amount of underground mine data, the network geometry could be reconstructed with a general resolution of the order of a few metres. This reconstruction is part of a larger project carried out with the aim to identify the chemical evolution of ore fluids through space and time, and the mechanisms of gold precipitation at Sigma (Garofalo 2000; available at the following URL: http://e-collection.ethbib.ethz.ch/cgi-bin/show.pl?type=diss&nr=13952). The 3D reconstruction shown here has allowed the recognition of some key geometrical and topological characteristics of the gold-bearing veins. Also, it has been used to estimate the total vein volume and mass input of B (as tourmaline) and quartz into the veins.

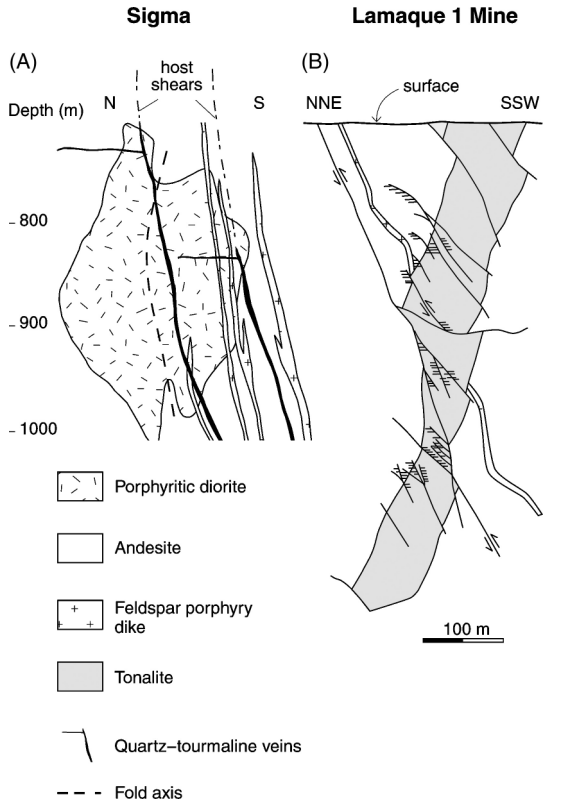

Fig. 1. Large-scale features of the Sigma (A, vertical section: 4950 E, no vertical scale exaggeration) and Lamaque (B, from Robert 1990) mines. In these deposits, shear zone-hosted, steeply dipping, quartz–tourmaline veins and associated subhorizontal veins crosscut a sequence of porphyritic diorite, andesites and feldspar porphyry dikes (Sigma) or tonalite plugs (Lamaque). The vein thickness is exaggerated. The sets of veins of the two deposits are in physical continuity, and their similarity is evident. In particular, at Lamaque, subhorizontal veins occur close to the footwall at upper terminations of shear zones and in the hanging wall at lower terminations of shear zones.

GEOLOGY OF THE SIGMA DEPOSIT

Here we summarize the most common features of the intensely studied Sigma deposit, and provide some additional data based on our geometrical study. More details on the geology of the area, the characteristics of hydrothermal alteration, the ages of host rocks and mineralization and the proposed genesis of the quartz–tourmaline veins are found elsewhere (Boullier & Robert 1992; Burrows & Spooner 1989; Claoué-Long *et al.* 1990; Daigneault 1983; Gaboury *et al.* 2001; Garofalo 2000; Garofalo *et al.* 1997a, 1997b; Jemielita *et al.* 1989; Kerrich & King 1993; Ludden *et al.* 1984; Matthäi & Garofalo 1999; Robert & Brown 1984, 1986a, 1986b; Robert & Kelly 1987; Robert *et al.* 1995; Wong *et al.* 1991).

The Archaean Sigma deposit is made up of a vertically extensive network of shear zone-hosted, quartz–tourmaline–gold veins formed during syntectonic hydrothermal activity. The veins crosscut a sequence of steeply dipping metavolcanic, plutonic and volcanoclastic rocks of the Abitibi greenstone belt of Canada (Robert & Brown 1986a), forming a network that extends to the south into the Lamaque deposit (Fig. 1). The part of the vein network that extends onto the Lamaque property is volumetrically smaller than Sigma, and was not well accessible for mapping during the course of this study. In the following, we briefly report the similarities between Sigma and Lamaque, but focus on our more detailed observations on the Sigma deposit.

From the Sigma–Lamaque vein network, about 270 tonnes(t) of gold have been extracted (Bédard 1976; Robert & Brown 1986a), a large production that makes this vein system a world-class deposit (Robert & Poulsen 1997).

Sigma–Lamaque belongs to a group of approximately 40 vein deposits of the Abitibi greenstone belt characterized by the presence of tourmaline as a major vein mineral (Robert 1994). These deposits formed around a large quartz–diorite to diorite sill intrusion (the Bourlamaque intrusion), occur close to a transpressional shear zone of regional importance,

known as the Cadillac tectonic zone (Robert 1989), and are bound by kilometre-scale shear zones often outcropping within the deposits (Robert 1990). At Sigma, the vein network has a minimum vertical dimension of 1.8 km and crosscuts a sequence of andesitic volcanics intruded by porphyritic diorite and feldspar porphyry dikes (Fig. 1A). At Lamaque, exploitable mineralization is restricted to a depth of approximately 1.2 km. Pyroclastic rocks of intermediate composition are present to the north and south of Sigma (Robert & Brown 1986a), and are tectonically juxtaposed against the mine sequence by two kilometre-scale, mostly planar and subvertical, E–W-striking shear zones, known as the North and South shears. Porphyritic diorite intruded the volcanic rocks and is preserved as characteristic elliptical bodies that resulted from shearing and transpositional folding (Fig. 1A). The proportion of porphyritic diorite increases steadily with depth, and a porphyritic diorite intrusion also occurs in the centre of the adjacent Lamaque mine (Daigneault 1983). Feldspar porphyry dikes crosscut the andesitic volcanics and porphyritic diorite (Fig. 1A), forming a network of conjugate, steeply dipping, tabular bodies striking east-west (E–W), eastnortheast-westsouthwest (ENE–WSW) and westnorthwest-eastsoutheast (WNW–ESE). Recent work by Gaboury *et al.* (2001) on the shallowest portion of Sigma shows that these dikes occur along two groups of swarms located to the north and south of the central diorite intrusion (see fig. 2 in Gaboury *et al.* 2001). Mutual crosscutting relations between porphyry dikes and the shear zone network show that their emplacement was broadly coeval with deformation (Garofalo 2000).

An anastomosing network of vertically extensive, south-dipping shear zones contains most of the quartz–tourmaline veins (Figs 1 and 2). These two minerals occupy more than 95% of the vein volume, with calcite, scheelite, albite, K-feldspar, sericite, biotite, chlorite, epidote, apatite, pyrite, pyrrhotite, chalcopyrite and gold present as minor phases. Discontinuous veins with the same mineralogy occur within the porphyry dikes ('dike stringers' of Robert & Brown 1986a), and in some places represent an important source of mineralization. Their geometry could not be constrained in this study; hence, our observations apply only to the shear-hosted veins.

The contemporaneous boudinage, drag folding, fracturing and brecciation of the material within the shear zones (Fig. 3) show that steep veins formed in a brittle–ductile regime (Garofalo 2000; Robert 1990; Robert & Brown 1986a). Three sets of shear zones form the anastomosing network, and strike E–W, WNW–ESE and ENE–WSW, the last of which hosts only thin and discontinuous veins (Fig. 2). Shear zones are vertically (Figs 1 and 3) and horizontally (Fig. 2) continuous, with vertical and lateral dimensions exceeding 1 km and a maximum thickness of 4–5 m. Steep veins are discontinuous along dip (Fig. 3) and strike (Fig. 2), with thicker and more continuous segments occurring where strike deviates to the south from E–W. Straight segments of the shear zones host thinner and more discontinuous quartz–tourmaline veins. As shown below, the anastomosing and segmented nature of the veins and the small-scale changes of their thickness within shears have a strong influence on gold grade distribution.

Robert & Brown (1986a; fig. 5b) measured the dips of the internal foliation of the host shears: these ranged from 80° to the south to 80° to the north, indicating a sinusoidal cross-sectional shape of the shear zones (see also Fig. 3). Most of the stretching lineations of the minerals in the foliation planes plunge from 80° to the east to vertical (see fig. 5d in Robert & Brown 1986a). These authors used these and other structural data to argue that, at Sigma, shear zones accommodated reverse subvertical movements occurring during N–S compression of the mineralized block of rocks. However, steep plunges of mineral lineations are found in ductile transpressional shear zones (Teyssier & Tikoff 1999; Tikoff & Greene

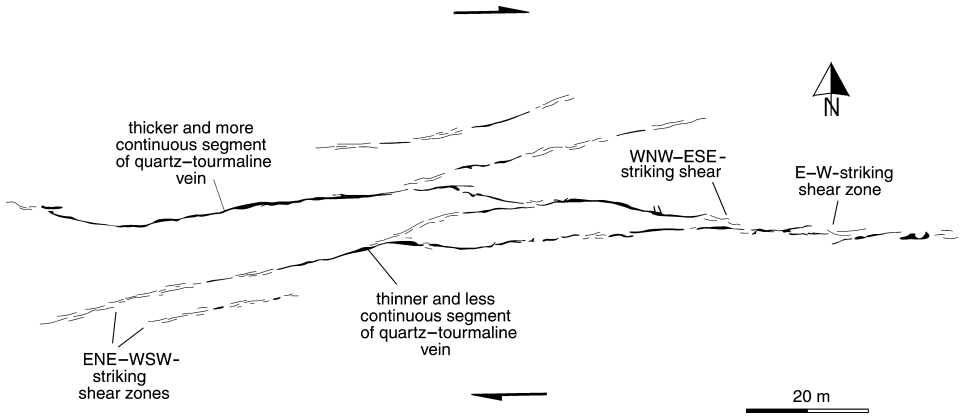

Fig. 2. Representative plan view of steep quartz–tourmaline veins and host shear zones at Sigma (26th level; mine coordinates: N, 1700 m; E, 1675 m; depth, 1050 m). The shear zone network is anastomosing, made up of interconnected E–W-, ENE–WSW- and WNW–ESE-striking sets. Vein thickness varies on the metre scale, but thicker and more continuous vein segments are most abundant within the E–W- and WNW–ESE-striking shears. A dextral displacement component can locally be inferred from displacement indicators and explains the observed geometry of this horizontal section.

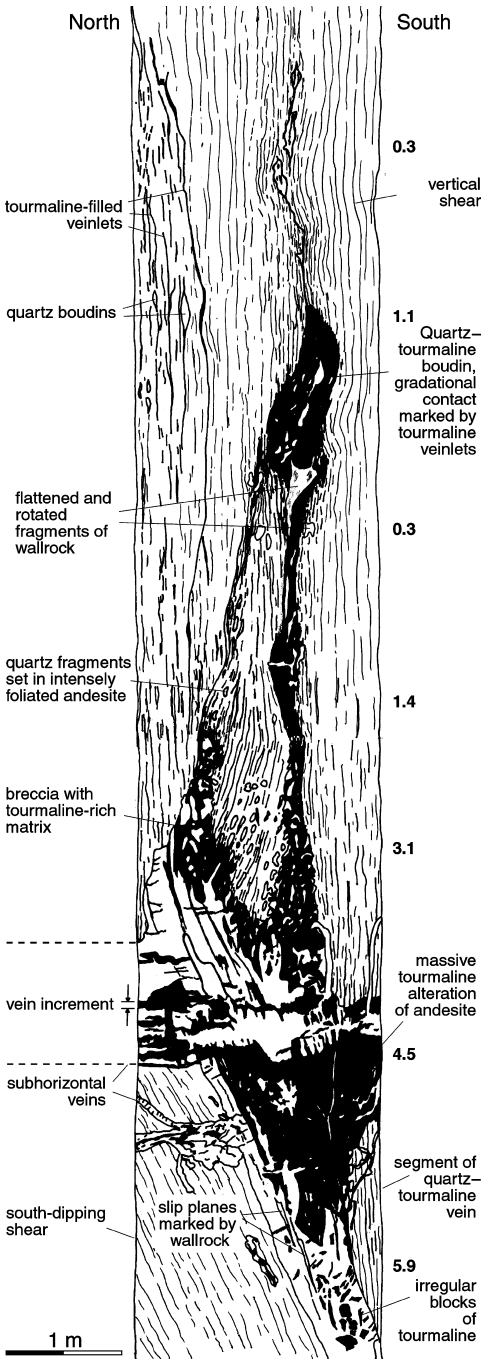

Fig. 3. Geometrical features of steep and subhorizontal quartz–tourmaline veins at Sigma. The width of the outcrop, 2 m, is that of the 18th–19th level raise (mine coordinates: N, 1570 m; E, 1600 m; depth, 690 m; lithology, andesite), which is cut perpendicular to the strike of the host shear. A segment of a steep vein terminates with a zone of intense brecciation within the host shear and intense tourmalinization of the andesite wallrock. Boudins of quartz–tourmaline vein occur at the top of this segment, and another segment of this vein is present immediately above the mapped area, showing that this is not a vein termination, but a shallower dipping shear segment. The average gold grade of the steep vein (in grams per ton, numbers on the right) is high at the vein segment tip and decreases sharply above. A subhorizontal vein connects at both sides of the tip of the steep vein, with several subparallel tourmaline levels marking the different vein growth increments.

1997), and are explained as the result of vertical extrusion and flattening of material within the zone. Steep plunges of lineations were described by Robin & Cruden (1994) for certain sections of the Cadillac tectonic zone about 180 km from Sigma. Very close to Sigma, Robert (1989) interpreted steep stretching lineations, obliquity of foliation and shear sense indicators of the Cadillac tectonic zone as evidence for dextral transpression. Furthermore, kinematic indicators for kilometre-scale shear zones close to Sigma show oblique-slip movements (Robert 1990; fig. 5D), sometimes complicated by complex reactivation histories. Hence, a strike-slip component of deformation might have been active at Sigma, and possible indications of the presence of this component in the host shears are given by: (i) the average dips of the shear zones, which are inconsistent (i.e. $>60^{\circ}$) with purely reverse movements and contemporaneous vein dilatancy; (ii) the anastomosing pattern of these zones along horizontal sections (Fig. 2), with strike directions consistent with a dextral strike-slip component of movement (Silvester 1988); and (iii) the presence of extensional veins splaying off the North shear that are inconsistent with purely reverse movements (Garofalo 2000). A strike-slip component of movement has also been used by Gaboury *et al.* (2001) to explain the geometry of some vertical veins present in the shallow portion of the deposit.

Gold-rich subhorizontal extension veins occur commonly at, or close to, the tips of segments of steep veins both at Sigma and Lamaque, and are characterized by open-space-filling textures (Fig. 3, see also fig. 10 of Gaboury *et al.* 2001). In plan view, these veins show a disc shape with average dimensions of the order of tens of metres (with maximum dimensions up to about 300×80 m), and some of them crosscut neighbouring steep veins. The dimensions and thickness of subhorizontal veins decrease with depth and, at a depth greater than about 950 m, they are so small that mining is uneconomical (C. Pelletier, personal communication, 1996). At Lamaque, subhorizontal veins occur near the footwall of the upper terminations of steep veins, or close to the hanging wall of the lower terminations of steep veins (Fig. 1B). At Sigma, subhorizontal veins occur at one or both sides of the tips of segments of steep veins (Fig. 3), with stacks of quartz and tourmaline fibres showing repeated opening events. This occurrence at the tips of vein segments is rarely evident in deposit-scale reconstructions (see, for example, fig. 3 in Robert & Brown 1986a) because of the segmented nature of the Sigma vein network. We interpret the subhorizontal veins as the result of the accommodation of shear displacement at the tips of steep vein segments. Here, a combination of reverse and strike-slip movements of the host shears might have induced a mixed-mode loading (Cooke & Pollard 1996; Pollard & Segall 1987) of the steep veins, which was resolved by the opening of the subhorizontal veins (see Barquins & Petit 1992, Bürgmann & Pollard 1994 and Petit & Mattauer 1995 on the formation of splay cracks or joints).

Finally, evidence for repeated opening of the subhorizontal veins during episodic slip of the host shear suggests an overall quasi-stationary permeability creation mechanism during dilation, which fostered vein formation only within specific shear zones and at their tips.

MINE DATABASE AND METHOD USED FOR THE COMPILATION OF CONSTRAINT POINTS

The underground mine database of the Sigma deposit represents the bulk of the geological data on which the present study is based. Outcrop mapping provides additional data on the detailed geometry of veins and the patterns of hydrothermal alteration. Built over more than six decades of underground activity (see Robert & Brown 1986a; Spooner & Barrie 1993), the database of this deposit consists of 40 level plans, more than 17 000 borehole logs and a large number of vertical sections, stope plans, raise maps, horizontal vein plans and gold grade plans. The Sigma mine has an E–W dimension of *c.* 2100 m, a N–S extension of *c.* 700 m and covers a total vertical interval of *c.* 1800 m (Fig. 4). These dimensions correspond to a volume of 2.57 km^3 (Table 1). We report the network geometry and gold grade distribution for a subvolume of the mine (Fig. 4) with an E–W dimension of 1380 m, a N–S dimension of 400 m and a vertical extent of 790 m. This subvolume is located between the 17th and the 34th mine levels and has a volume of about 0.44 km^3 (Table 1).

At Sigma, plans and longitudinal sections (compiled at a scale of 1 : 360) constitute the basis for resource evaluation during mining (Fig. 5, see also Fig. 2). Stope and level plans report the detailed vein geometry at any given level ('roof' and wall mapping) and contain a large amount of geological information. In these plans, changes in attitude of the veins along strike are captured with a resolution of 2–3 m or better, and thickness is constrained to at least 25–30 cm (Fig. 5). The large number of borehole logs and level plans are used to build a set of regularly spaced (one every 150 ft), N–S-orientated, vertical sections. These sections include a two-dimensional (2D) geological interpretation of the deposit and are used here to constrain the 3D characteristics of the veins to within 5 m along dip. This constraint provides a high

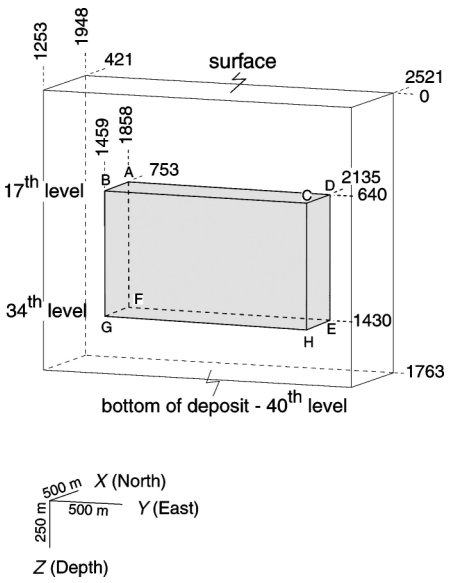

Fig. 4. To-scale representation of the total mined rock volume at the Sigma deposit and of the studied subvolume (highlighted) for which the reconstruction was performed. The axes *X*, *Y* and *Z* correspond to the north, east and vertical directions. The coordinates of the corners of the volumes are reported in metres. The subset contains most of the vein network occurring between the 17th and 34th levels.

Table 1 Calculated and estimated volume characteristics of the Sigma deposit.

	Measured volume (10^6 m^3)	Total deposit estimated (10^6 m^3)	10^5 t in deposit*
Deposit	435.0	2572.5	
Vein network total	0.9	5.5†	
Vein tourmaline	0.4‡	2.1†	65
Vein quartz	0.5	3.2	84
Vein carbonate§	0.05	0.3	7.5
Boron			0.7
Gold¶			0.003

*Tonnage calculated using the following density values (Deer *et al*. 1992): quartz, 2.65 g cm^{-3}; carbonate, 2.70 g cm^{-3}; tourmaline, 3.09 g cm^{-3}. Tourmaline density has been calculated on the basis of the average composition of vein tourmaline (Robert 1983).

†Calculated assuming that observations in the measured subset volume are representative for the entire deposit volume.

‡Calculations based on image analysis data.

§Based on maximum volumetric estimation of 5% (Robert & Brown 1986a).

¶Cumulated gold production of Sigma and Lamaque taken from Robert & Brown (1986a) and Bédard (1976)

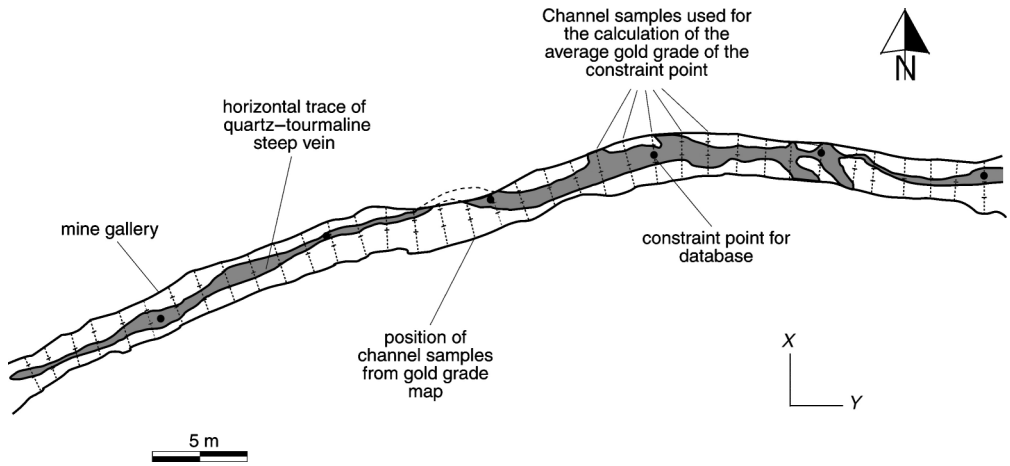

Fig. 5. Composite diagram showing the geological information for one of the subparallel steep veins of the Sigma mine (23rd level plan; gallery, 2304 W; depth, 914 m) including gold grades. All level plans of the deposit report the geometry of the vertical veins and have an average vertical interval of 45 m (see also Fig. 6B). More than 17 000 diamond drill holes provide additional geometrical information between mine levels and also to the east and west of the studied subset. The dots at the centre of the vein represent constraint points used in the reconstruction. The positions of the channel samples in the gold grade plan are reported as dotted lines across the gallery. These samples are *c.* 3.0 m in width (i.e. total gallery width), are divided into two or three segments, and are collected with a 1.5–2.0-m spacing along vein strike. In the compilation, only segments that report the gold grade of vein and immediately adjacent wallrock were considered. To smooth gold grade in the veins, an average value for each database point was calculated using the mean vein gold grade values of five channel samples adjacent to the measuring point. These samples include the one closest to the measurement point and two other neighbouring samples from either sides of the measurement point.

geometrical control on the data set presented below; hence, the geometrical reconstruction shown here can be considered to be sufficiently determined at the large scale. The geometrical data on the horizontal extension veins are somewhat less precise. This is due to the fact that only subhorizontal veins with a horizontal dimension larger than 100 m were excavated and separately reported in the 2D sections. Because of this incompleteness, horizontal veins are not included in the 3D representation of the vein network, but their structural relationship with the subvertical veins is reported using 2D sections where appropriate.

Gold grade distribution within the network is recorded in gold grade and stope plans, which compile Au concentrations (weighted by sample length) in channel samples collected every 1.5–2 m along vein strike. Spatially discontinuous data depict gold distribution in the stopes, but detailed control of the grade is achieved along the main galleries of the mine (Fig. 5), where veins are continuously exposed along strike. Along these galleries, gold concentrations are systematically reported for segments of channel samples that take into account the vein and the immediately adjacent wallrock. Hence, these plans allow a resolution of along-strike changes in gold grade distribution of about 2 m.

Our reconstruction of geometry and gold grade distribution uses a regularly spaced array of constraint points located at the centre of the subvertical veins reported in the level plans (Fig. 5). The 3D coordinates, vein thickness and gold grade of each constraint point were extracted from the mine database and compiled for the subvolume shown in Fig. 4. A spacing of 9 m (i.e. 30 ft, Fig. 5) between these points along vein strike was found to be sufficient to capture strike and thickness changes of the veins. Care was taken to identify the positions of the vein tips of each horizontal trace of the steep veins. The geometrical position of the vein tips was placed where the vein thickness diminished below 5 cm. A total number of 2838 constraint points was compiled to define the 3D geometry of the veins (Fig. 6 and electronic data repository is available on request). The density of these data points (compare the two perspective views of Fig. 6) alludes to the geometrical complexity of the vein network.

RECONSTRUCTION OF THE 3D GEOMETRY OF SINGLE VEINS

The reconstructions were carried out with the software GOCAD®, a computer application that allows the interactive creation, editing, integration, visualization and export of geological objects in three dimensions. GOCAD® provides an algorithm called 'discrete smooth interpolation' (Mallet 1992), which is used on any type of 2D or 3D mesh (i.e. a patchwork of simple geometrical objects that approximate a complex shape). This algorithm efficiently interpolates attribute values at data points (thickness and gold grades in our case) using a robust criterion that eliminates attribute discontinuities across mesh nodes and honours specific fitting

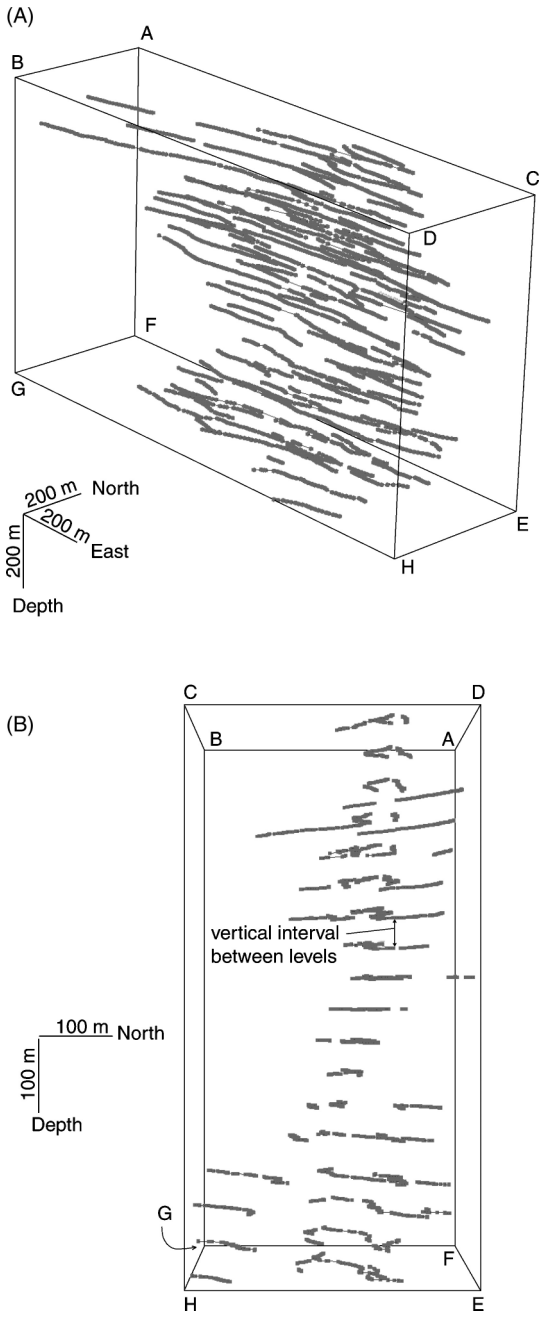

Fig. 6. Three-dimensional distribution of the constraint points in the studied subvolume of the deposit (refer also to Fig. 4). Every line of points corresponds to the trace of a vein on a mine level. The perspective view from ESE (A) highlights the density of the data points within the subset, whilst the view from the E (B) shows the spacing of these points within the subset.

constraints (see, for example, Segonds *et al.* 1997). More details on the characteristics of GOCAD® and on its use in different research topics can be found at the following web site: http://www.ensg.u-nancy.fr/GOCAD.

The internal geometry of each vein has been reconstructed using 3D triangular meshes, each one including the changes in strike or vein discontinuity reported in the database. The distance between mesh nodes was set between 2 and 20 m, which was sufficient to honour the small-scale changes of vein properties in the reconstructions.

Fifty-three steep veins contained within 12 distinct, vertically extensive shear zones have been singled out with the available mine database via the identification of their tip lines, linkage and discontinuity across different mine levels, and then reconstructed using the compiled constraint points. The 3D reconstruction of vein geometry is based on three successive steps as summarized in Fig. 7. Figure 7(A) shows the database points of an array of steep veins intersected at each mine level in the deposit from a depth of 640 m to 960 m. For the 3D reconstruction, the tip points of each horizontal vein trace have been used as a geometrical 'anchor point' to define the 3D tip line of the veins (Fig. 7B). A smooth surface was eventually fitted with GOCAD®, matching tip line and constraint points to represent the 3D geometry of each vein (Fig. 7C). Thus, the reconstructed shape of each single vein represents the best-fit smooth surface through the corresponding array of constraint points. Such interpolation does not produce artificial surface oscillations, as would be the case for polynomial interpolation, and results in an accurate fit of the database points. Vein thickness and gold grade are mapped on the reconstructed surfaces using different graphical symxbols. Contouring and colour coding are used to show the interpolated vein thickness in centimetres and gold grades in grams per ton ($g\,t^{-1}$), respectively. It should be noted that shapes defined by thickness and gold grade contours on the vein surfaces cannot be modified by the use of a larger number of constraint points in the database. This shows that the use of a larger database would result in a higher resolution of the reconstructed vein geometry and gold grade distribution (especially along the vertical direction), but would not modify the shapes reconstructed here.

Veins continuing beyond the reconstructed rock volume were terminated at the top and bottom of the studied block. Changes in vein orientation are shown as surface bends, and areas of relatively low thickness (< 50 cm) correspond to discontinuous portions of veins hosted by straight portions of shear zones (compare with Fig. 2). Changes in gold grade are recorded as variations of colour tones superimposed onto the thickness contouring. This simultaneous representation of different spatial variables on a vein allows the visual correlation between the large-scale geometrical properties of the vein network and its gold grade distribution.

COMPOSITE VEIN VOLUME AND FRACTION OF VEIN TOURMALINE

The calculation of steep vein volumes is possible using the interpolated thickness values for each vein. Volumes have

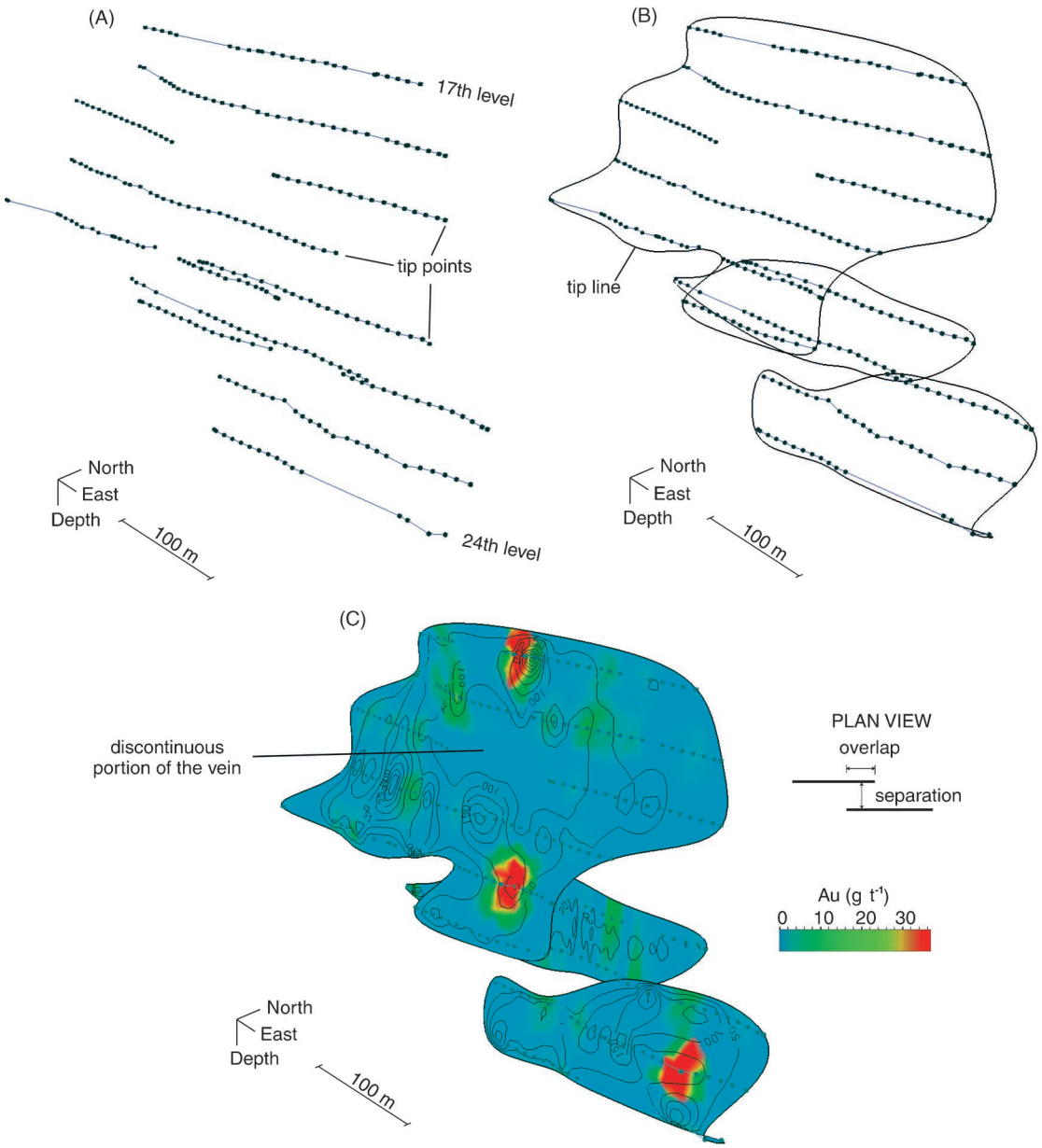

Fig. 7. Technique used to reconstruct the three-dimensional (3D) geometry of three vertical veins (L zone in the mine). (A) Veins are singled out using the geological interpretation available in the mine database. The tip lines of the veins are identified by fitting a smooth curve through the tip points at each mine level. (B) Tip lines are used as geometrical constraints for the reconstruction of the 3D geometry of the veins. The 3D geometry of each vein is built as a best fit of a surface through the tip line and constraint points. (C) Vein thickness and gold grades are represented as surface properties. Overlap and separation of the vein segments are measured on a horizontal plane (see lateral inset). Vein thickness is contoured in centimetres, and gold grade in grams per ton ($g\,t^{-1}$) is colour coded.

been created with GOCAD®, expanding the vein surfaces (Fig. 8A) along two surface-normal vectors by a distance equal to half of the vein thickness (Fig. 8B). The two resulting surfaces were taken as the envelope of the vein volume and merged together to build discrete vein volumes (Fig. 8C). The vein volume histogram (Fig. 8D) shows that most of the steep veins do not exceed $1000\,m^3$. The total volume of the reconstructed vein network is about $0.9 \times 10^6\,m^3$ (Table 1). Assuming that the vein density in the studied rock volume is representative of the whole deposit, the total volume of the vein network is estimated as $5.5 \times 10^6\,m^3$ (Table 1).

The average abundance of tourmaline in the veins has been estimated using image analyses of 46 underground photographs of steep and subhorizontal veins from eight different mine locations spanning a vertical interval of 875 m. The thresholding analysis mode of the public domain program 'Scion Image for Windows' (National Institute of Health

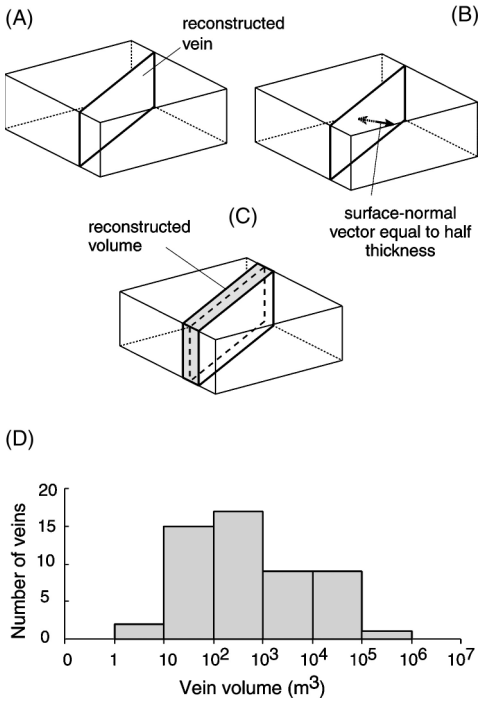

Fig. 8. Schematic representation of the method used to build the vein volumes. (A) Vein surfaces and their thickness distribution constitute the geometrical input for the reconstruction of the vein volumes. (B) Using the mesh nodes of the reconstructed veins, each surface is diametrically expanded by a distance equal to half the vein thickness along the vein normal vectors. (C) The vein volume is built merging together the expanded surfaces. (D) Distribution of the calculated volumes for the reconstructed single veins.

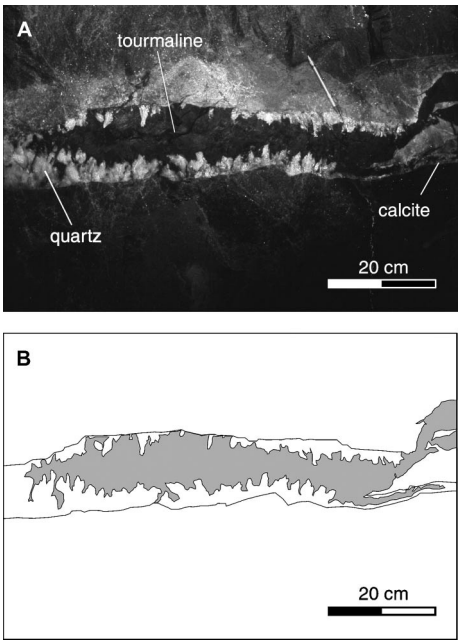

Fig. 9. Analysis of the area occupied by tourmaline in a digital image of a quartz–tourmaline vein (A, 32nd crosscut; depth, 1338 m). The area is automatically identified (grey area in B) using a 'density slice' thresholding mode. Given the high colour contrast between tourmaline and the other vein minerals, this analysis is accurate.

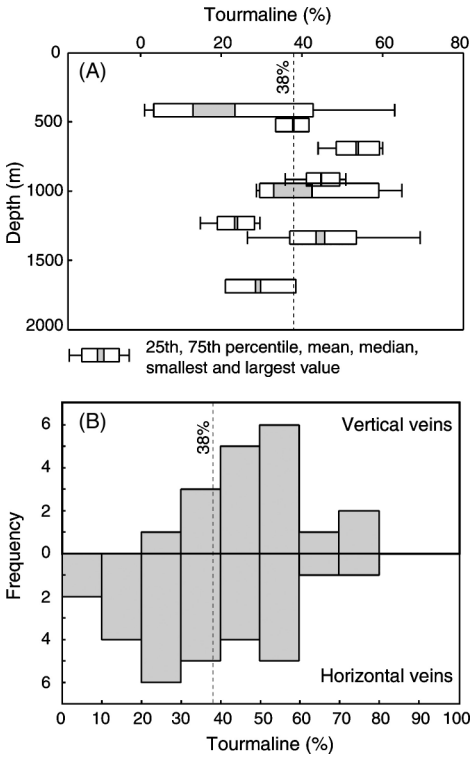

Fig. 10. Estimated tourmaline abundance within the gold-bearing veins of the Sigma deposit. (A) Box plot of the variation as a function of depth in the deposit. Smallest and largest observations are reported together with the quartiles. Several groups of images show a mean value between 20% and 50%. The average of the calculated means of all the groups is equal to 38%. (B) Comparison between the tourmaline distribution measured in vertical and horizontal veins. Apart from a larger spread of the values for the horizontal veins, there is no significant statistical difference between the two vein types in terms of tourmaline abundance.

1998) was used for the measurements. Figure 9 shows the accuracy of this method for the estimation of tourmaline abundance, and Fig. 10 reports the results of the calculated volumes as a function of deposit depth and vein type. Despite the large variation of tourmaline abundance in the veins, most of the measured values lie within the 20% and 50% intervals (Fig. 10A). Also, except for a relatively larger spread of values for the horizontal veins, the two types of veins show no statistical difference (Fig. 10B). This implies that a single representative value can be used as the tourmaline abundance. This average value is equal to 38% (Fig. 10A,B) and does not include the amount of tourmaline precipitated in the wallrocks as a result of fluid–rock interaction. The calculated tourmaline volume is therefore a minimum estimate of the amount of tourmaline precipitated in the Sigma vein network, and the actual value could be 1–2% larger (Garofalo 2000). The volumes occupied by tourmaline and quartz in the studied rock volume are about $0.4 \times 10^6\,m^3$ and $0.5 \times 10^6\,m^3$, respectively. This corresponds to $2.1 \times 10^6\,m^3$ of B and $3.2 \times 10^6\,m^3$ of SiO_2 in the entire

deposit (Table 1), which represent independent mass balance constraints to the Au-precipitating mechanism in the veins.

CHARACTERISTICS OF THE 3D VEIN NETWORK

The reconstructed 3D geometry and related gold grade distribution of the vein network are shown in Figs 11–16. Figure 11 is a perspective view from the south-east of the 10 largest veins, and Fig. 12 shows the along-strike view towards the west of all 53 reconstructed veins.

Throughout the following text, the 3D characteristics of the veins will be described using the terminology employed by Willemse *et al.* (1996) and Childs *et al.* (1995) for fault arrays. Vein 'height' and 'length' refer to the longest vein dimension measured down dip and along strike, respectively. An element of a discontinuous vein is called a 'vein segment', the 'aspect ratio' is defined as the ratio between the vein length and vein height, and a 'relay structure' is defined as the zone between the tips of two veins (with or without overlap).

The 3D reconstruction shows veins with an isometric shape (i.e. similar height and length, Fig. 12) and veins with a small height. An en echelon-like arrangement is more evident for veins with an isometric shape (Fig. 11) and less for veins with a variable shape. The spatial arrangement of the 10 largest veins of Fig. 11 is shown in Fig. 13(A), which correlates separation and overlap in metres (see Fig. 7C for a definition of these parameters and method of measurement). Vein overlap is proportional to separation and follows the trend reported by Aydin & Schultz (1990) as a typical feature of strike-slip echelon faults in a broad range of scales. The helicoidal and concave-upward shape observed in some large veins (Fig. 12) is considered to be a typical feature of Riedel-type shears in natural strike-slip fault networks (Silvester 1988) and sand box experiments (Naylor *et al.* 1986). These features have also been reported by Gaboury *et al.* (2001) in the shallowest portion of the vein network of Sigma.

In the reconstructed subvolume, the dimensions of a few vertically extensive veins exceed those of veins with a small height (Fig. 12). The small separation between vein segments in the network brings about a graphical superimposition in the 3D representation, and the few large veins hide many

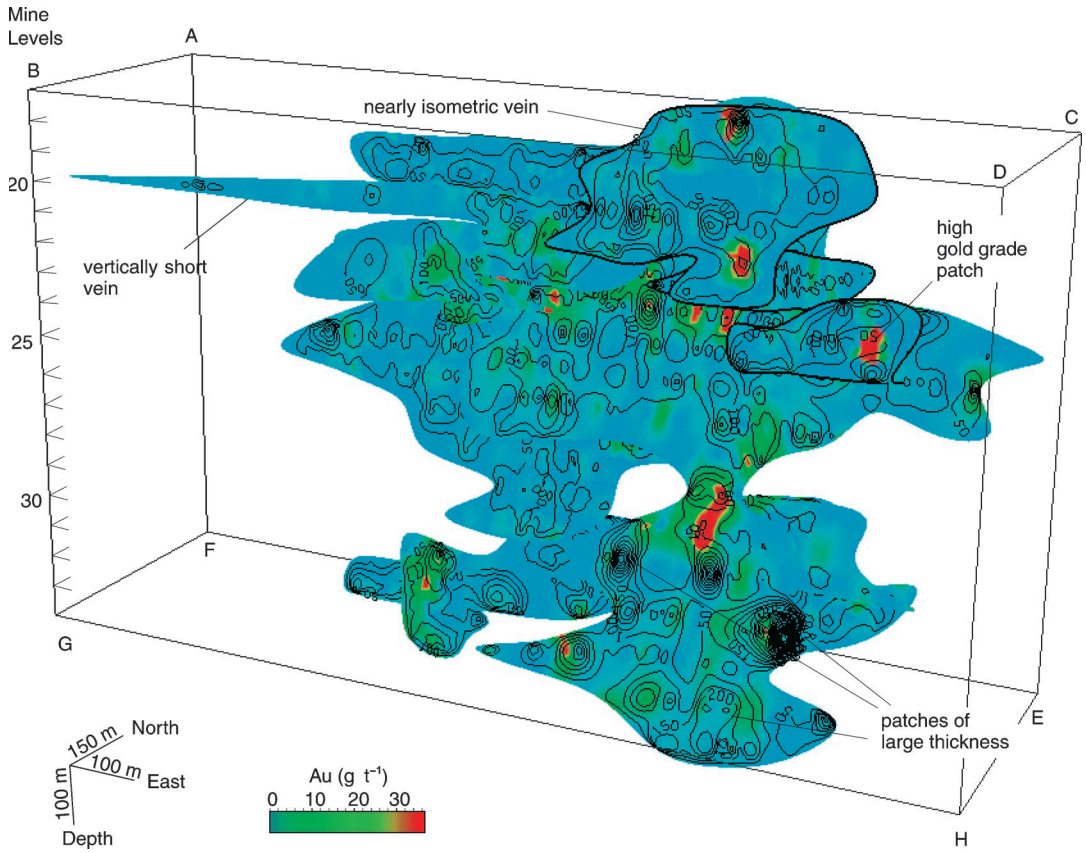

Fig. 11. Perspective view from the south-east of the steeply dipping veins reconstructed in this study. Veins with a vertical dimension exceeding that of the studied block are terminated slightly above or below the top or the bottom of the subset. The three veins reported in Fig. 7(C) and the mine levels are highlighted for reference. Vertically extensive veins have variable geometries. Their shapes range from nearly isometric to elliptical. Thick patches and gold-rich domains span more than one level of constraint points, ruling out the possibility that they are artefacts of the interpolation.

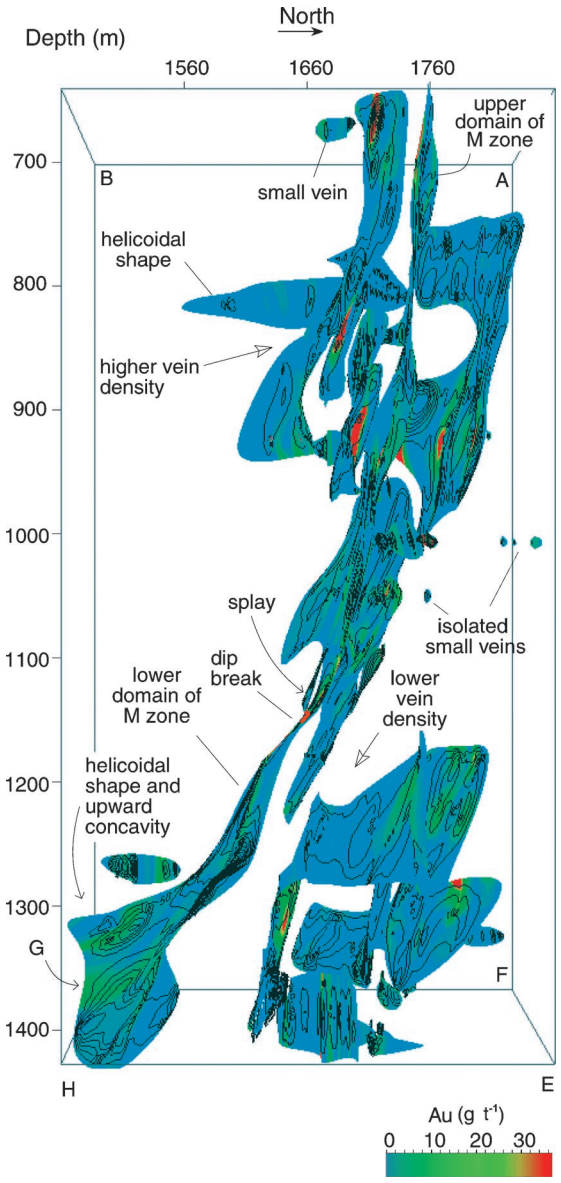

Fig. 12. Perspective view from the east of all reconstructed veins. The relatively small across-strike separation of vein segments leads to their graphical superimposition. As a result, large veins hide some small veins. Helicoidal shape and upward concavity are evident for two large veins. A vein zone spans the whole studied vertical interval. This vein (M zone in mine terminology) is characterized by the presence of a break in dip at a depth of *c.* 1140 m and a vertically short splay originating at this break. Isolated small veins generally have gold grades lower than those of the vertically extensive veins. Note also the strong variation of vein density within the subset.

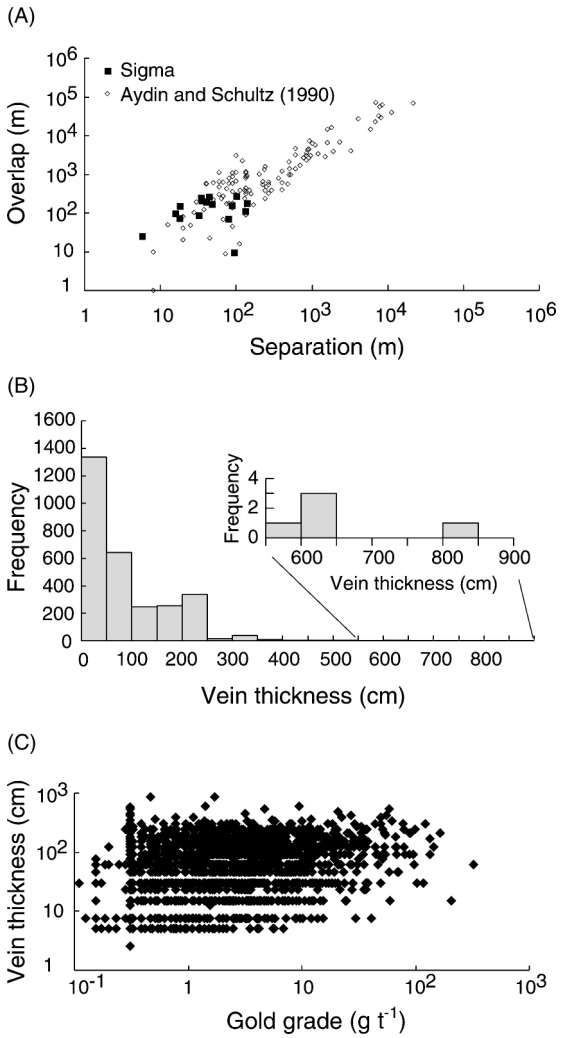

Fig. 13. (A) Overlap–separation plot for the steeply dipping veins. Parameters measured for vein pairs on a horizontal plane (average values are reported because veins are neither planar nor isometric in shape). Values show a moderate positive correlation between overlap and separation. (B) Histogram for the 2838 thickness constraints; 82% of the measured values fall below 1 m and a thickness larger than 3 m is rare. (C) Vein thickness–gold grade correlation for the 2838 constraint points.

small veins in Fig. 12. Thirty-seven veins in the network have a maximum height of about 100 m, and 34 of them have a volume of less than 1000 m^3 (Fig. 8D). These smaller veins either splay off extensive veins, or occur as isolated bodies (Figs 12, 15 and 16). Their real number at Sigma is certainly underestimated because of the geometrical resolution used for the reconstruction. Despite their much smaller height and length, vertically short veins have a thickness distribution that is indistinguishable from that of large veins. This is shown by the cumulative distribution of the 2838 thickness values compiled in this study, which is skewed towards a predominance of thinner veins (Fig. 13B), with 82% of the values less than 1 m. Thus, most of the veins have a similar thickness irrespective of their height or length, and this may be interpreted as an indication that the control mechanism for dilation in the host shear was identical throughout the deposit. This suggests that, at the time of vein formation at Sigma, relatively few, already closely spaced, large shears controlled

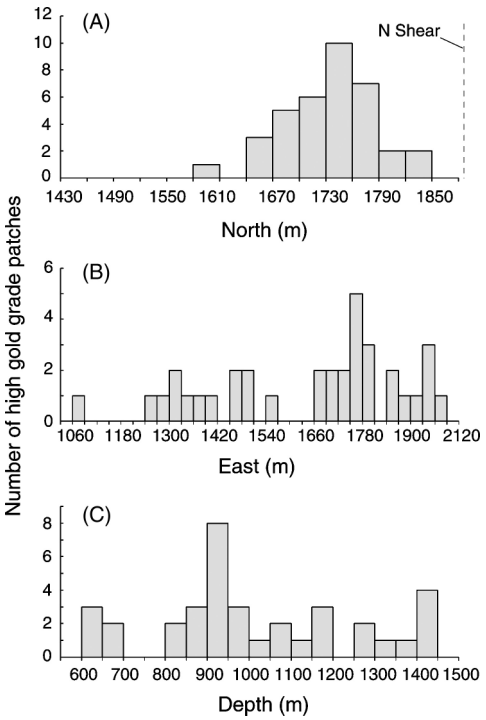

Fig. 14. Location of the centres of the gold-rich patches in the 10 vertically most extensive veins. Only the patches having grades higher than 25 g t^{-1} are plotted.

dilation and thus the permeability structure of the network, whilst small-scale veins only influenced local features. This is illustrated by the fact that the aggregated volume of the 10 largest veins (Fig. 11) equals 94% of the total calculated volume.

Vein thickness and gold grade within the network are neither uniform nor correlated with each other. In most of the reconstructed veins, large thickness and high gold grade areas are distributed along vertically elongated patches (Figs 11, 15 and 16). Within large veins, these patches are particularly well developed (Fig. 11), suggesting that their formation created stationary zones of high vein permeability within the network. These areas have a strike length ranging from 30 to 100 m, and horizontal distances between contiguous patches range from 50 to 120 m. Areas with very high gold grades (i.e. defined here as those in which the Au concentration in the veins exceeds 20 g t^{-1}) have strike lengths between 20 and 75 m, comparable to those of the thick patches. However, no correlation between gold grade and vein thickness is evident from the compiled data (Fig. 13C), and very high gold grades occur also where vein thickness is relatively low (Figs 11 and 15). In large veins, gold-rich patches extend across different mine levels, showing that their shape is not an artefact of the interpolation. The spatial distribution of the centres of the richest patches is reported in Fig. 14, where patch coordinates are plotted individually in order to highlight potential clusters. Figure 14(A) shows that most of these areas are located within a 200-m-wide E–W corridor of high vein density over the depth interval of 600–950 m (Fig. 12). There is no clustering along this corridor or with depth (Fig. 14B,C).

One important characteristic of the reconstructed vein network is the presence of one continuous vein with a height equal to that of the studied rock volume (i.e. 790 m, Fig. 12). This vein, called the 'M zone' at Sigma, is an economically important element of the network and is best described as an interconnected array of steep veins rather than a single body. The height of the M zone exceeds the vertical extent of the studied subset, but its large-scale features are captured. Figure 12 shows a dip-angle break at a depth of *c.* 1140 m, below which a progressive decrease of vein density occurs and the cross-strike separation of the veins increases (compare with Fig. 2). As the M zone shares many geometric characteristics with all other large veins, we will use it as a proxy to characterize the geometry of the large veins and their gold grade distribution. Small veins will be described within the context of their role as specific network features.

One of the most prominent features of the M zone is its complex geometry (Fig. 15). Its maximum length reaches 850 m at a depth of 914 m (i.e. 23rd level) and the shortest is only 75 m (i.e. 28th level). As the geological database does not show any offset of an originally larger vein in this part of the deposit, this geometry is primary and cannot be attributed to any post-veining event. A variable aspect ratio is typical of all reconstructed veins, but shape irregularities are greatest in the M zone. Here, thick patches are continuous up to 200 m in height (i.e. across five mine levels), but have a much smaller length ranging from 20 to 100 m. This vertically elongated arrangement probably reflects steps in the anastomosing host shear zones (compare with Fig. 2), and cannot be explained by bias in the smooth interpolation of the data values. The dip break (Fig. 15) marks a major discontinuity for these patches and corresponds to the interconnection of two south-dipping vein domains (Fig. 12). This geometry may suggest independent growth of the two domains, whereby the shallow and deep domains propagated independently and then connected at some stage of the network evolution.

An exceptionally gold-rich area occurs at the dip break of the M zone (Figs 12 and 15). An E–W-striking, vertically short, gold-rich splay with a dip angle exceeding that of the M zone connects in this area (inset GH of Fig. 15), emphasizing how important vein interconnections are for fluid flow and gold deposition at Sigma. Other interconnections with similar splays are reported in the two insets of Fig. 15. Two vertical sections and one horizontal section across gold-rich areas show additional geological detail that is not part of the 3D reconstruction. The insets AB and CD show a 50-m-high and 170-m-long steep splay connecting at its two

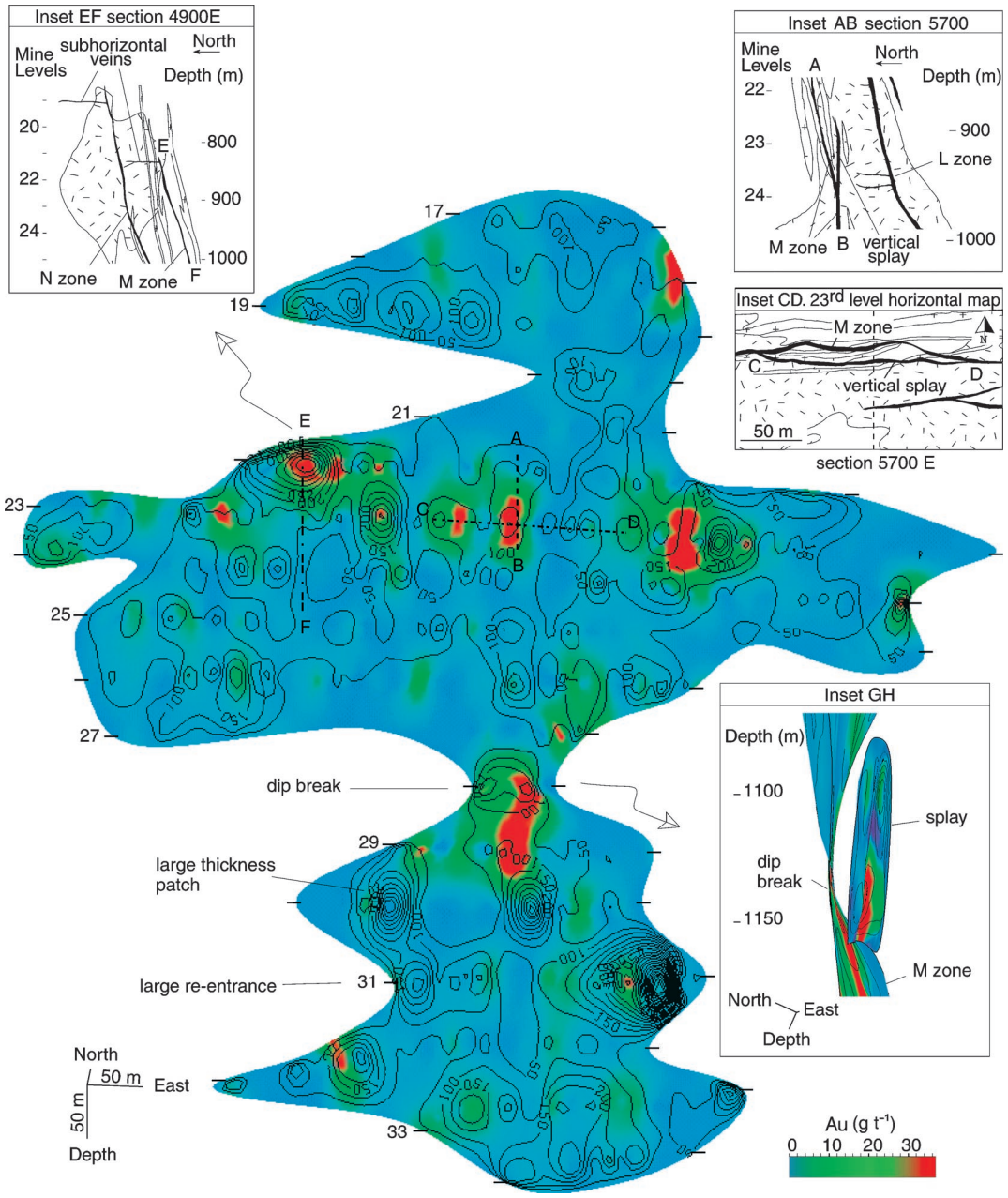

Fig. 15. Perspective view of the M zone from the south. Mine levels are marked at the vein tip for reference. Colour shading and thickness contouring reveal the patchy distribution of gold-rich areas and thick vein portions. High gold grades are poorly correlated with vein thickness, but correspond to features such as the dip break, vertical splays and branching of subhorizontal veins. Inset GH: view from the east of the dip break and associated vertical splay. Here, the M zone has a dip that is less than that of the splay. Insets AB and CD: vertical and horizontal sections through several gold-rich patches occurring in the shallower part of the M zone at a bifurcation of the vein. Inset EF: vertical section through the tip of the M zone in a gold-rich patch. In all insets, the vein thickness is exaggerated and rock symxbols are as in Fig. 1.

ends (points C and D) with the M zone. The interconnection with this splay (i.e. a branch line) lies slightly below the centres of the three gold-rich areas intersected by the line CD (inset AB of Fig. 15). The high gold grade patch cut by section EF is located close to the intersection with a subhorizontal vein splaying off the tip of the M zone (see Figs 1A and 15). Other vein interconnections show similar gold-rich areas within the network. Vertically short splays with high dip angles are present in several other large veins (Fig. 16), indicating development in a dextral strike-slip regime. Thus, vein branching played a decisive role in the location of gold-rich patches, sometimes even evident at the metre scale (Fig. 3).

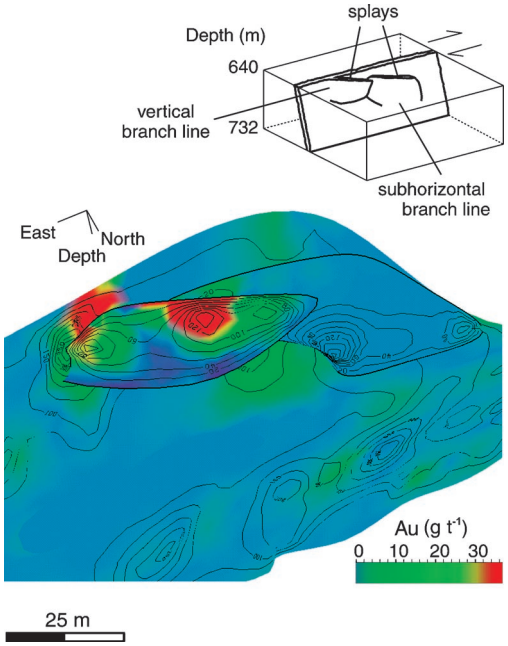

Fig. 16. View from the north of two splays originating at different levels from a vertically extensive vein (i.e. largest vein in Fig. 7C). A block diagram shows the relations between splays and mineralized shear.

CONCLUSIONS

(1) Large collections of underground mine data allow detailed studies of vein networks. In the Sigma mine, an array of 2838 regularly spaced constraint points was used to reconstruct the 3D geometry and the gold grade distribution of 53 veins contained in a representative portion of the Au-mineralized, quartz–tourmaline vein network.

(2) Our reconstruction identifies a few steeply dipping, vertically extensive veins and a large number of vertically short veins in the network. The geometrical characteristics and the arrangement of the largest veins are consistent with those of strike-slip fault systems. Vertically extensive veins are made up of the coalescence of different domains developed within steeply dipping, E–W-, ENE–WSW- and WNW–ESE-striking brittle–ductile shear zones. Their geometry is characterized by sinusoidal and helicoidal shape, and large changes of their aspect ratio. From the compiled database, we could not discriminate the absolute thickness of vertically short veins from that of large veins. This suggests that most vertical veins formed simultaneously in the network, but only a few of them interconnected to form vertically continuous zones. Vertically short veins are either isolated or splay off the larger veins with a high dip angle.

(3) In the vertically extensive veins, the thickest areas are vertically elongated and may extend for hundreds of metres in the vertical dimension. These areas occur as patches with a strike length ranging from 30 to 100 m. They are typical features and presumably represent stationary areas of high permeability within the vein network. The gold grade distribution within the veins is also patchy, and there is no correlation between thickness and gold concentration in the veins. The highest gold grades are instead located at interconnections between large veins and small splays, and at intersections between large veins and subhorizontal veins.

(4) Large veins make up most of the network volume, and represent the most important ore body. Volumetric estimates based on the 3D reconstruction represent an important independent mass balance constraint for the deposit. They have been combined with thresholding image analysis of underground photographs of veins in order to estimate the amount of tourmaline and quartz precipitated within the network at Sigma. We calculate that $2.1 \times 10^6\,m^3$ of tourmaline and $3.2 \times 10^6\,m^3$ of quartz precipitated in the veins during gold deposition.

ACKNOWLEDGEMENTS

The authors thank Philippe Renard for his help with the use of GOCAD® at Eidgenössische Technische Hochschule (ETH) Zürich. We also wish to thank F. Robert for the constructive discussions at the Sigma mine during an early stage of this project. Funding from the ETH Zürich, the Schweizerische Nationalfond (project number 20-52265.97) and Placer Dome Ltd. is gratefully acknowledged. F. Robert and an anonymous reviewer improved the content of the original manuscript.

REFERENCES

Aydin A, Schultz RA (1990) Effect of mechanical interaction on the development of strike-slip faults with echelon patterns. *Journal of Structural Geology*, **12**, 123–9.

Barquins M, Petit J-P (1992) Kinetic instabilities during the propagation of a branch crack: effects of loading conditions and internal pressure. *Journal of Structural Geology*, **14**, 893–903.

Bédard P (1976) *The Lamaque Mine*, pp. 118–24. Ministère des Richesses Naturelle, Direction Gènèrelle des Mines, Montreal.

Boullier A-M, Robert F (1992) Paleoseismic events recorded in Archean gold–quartz vein networks, Val d'Or, Abitibi, Quebec, Canada. *Journal of Structural Geology*, **14**, 161–79.

Bürgmann R, Pollard DD (1994) Strain accommodation about strike-slip fault discontinuities in granitic rock under brittle-to-ductile conditions. *Journal of Structural Geology*, **16**, 1655–74.

Burrows DR, Spooner ETC (1989) Relationships between Archean gold quartz vein-shear zone mineralization and igneous intrusions in the Val d'Or and Timmins areas, Abitibi Subprovince, Canada. In: *The Geology of Gold Deposits: the Perspective in 1988* (eds Keys RR, Ramsay WRH, Groves DI), *Economic Geology Monograph*, **6**, pp. 424–44. The Economic Geology Publishing Co.

Childs C, Watterson J, Walsh JJ (1995) Fault overlap zones within developing normal-fault systems. *Journal of the Geological Society*, **152**, 535–49.

Claoué-Long JC, King RW, Kerrich R (1990) Archean hydrothermal zircon in the Abitibi greenstone belt: constrains on the timing of

gold mineralization. *Earth and Planetary Science Letters*, **98**, 109–28.

Cooke ML, Pollard DD (1996) Fracture propagation paths under mixed mode loading within rectangular blocks of polymethyl methacrylate. *Journal of Geophysical Research*, **101**, 3387–400.

Daigneault R (1983) Geologie et geochimie du gisement d'or de la mine Lamaque, Vald'Or Quebec. PhD. Ecole Polytechnique de Montreal, Montreal.

Fisher DM, Brantley SL, Everett M, Dzvonik J (1995) Cyclic fluid flow through a regionally extensive fracture network within the Kodiak accretionary prism. *Journal of Geophysical Research*, **100**, 12881–12894.

Gaboury D, Carrier A, Crevier M, Pelletier C, Sketchley DA (2001) Predictive distribution of fault-fill and extensional veins: example from the Sigma gold mine, Abitibi Subprovince, Canada. *Economic Geology*, **96**, 1397–405.

Garofalo P (2000) Gold precipitation and hydrothermal alteration during fluid flow through the vein network of the mesothermal gold deposit of Sigma (Abitibi belt, Canada). PhD. Swiss Federal Institute of Technology, Zurich.

Garofalo P, Heinrich CA, Ridley JR, Robert F (1997a) Advances in understanding hydrothermal alteration of the Sigma gold deposit, Val d'Or, Quebec, Canada. In: *EUG 9. European Union of Geoscience, Strasbourg, France* (ed Oxburgh RE), pp. 556. Cambridge Publications Limited, Cambridge, UK.

Garofalo P, Ridley JR, Heinrich CA (1997b) Variations in hydrothermal alteration at the Sigma gold deposit (Val d'Or — Quebec); are they relevant for understanding gold deposition?. In: *Mineral Deposits: Research and Exploration. Where Do They Meet?* (ed. Papunen H), pp. 193–6. Balkema, Rotterdam.

Jemielita RA, Davis DW, Krogh TE, Spooner ETC (1989) Chronological constraints on the origin of Archean lode gold deposits in the southern Superior Province from U/Pb isotopic analyses of hydrothermal rutile and titanite. In: *Geological Society of America 1989 Annual Meeting*, p. A351.

Jing L, Stephansson O (1997) Network topology and homogenization of fractured rocks. In: *Fluid Flow and Transport in Rocks. Mechanisms and Effects* (eds Jamtveit B, Yardley BWD), pp. 191–202. Chapman & Hall, London.

Kerrich R, King R (1993) Hydrothermal zircons and baddeleyite in Val d'Or Archean mesothermal gold deposit: characteristics, compositions, and fluid inclusion properties, with implications for timing of primary gold mineralization. *Canadian Journal of Earth Sciences*, **30**, 2334–51.

Ludden JN, Daigneault R, Robert F, Taylor RP (1984) Trace element mobility in alteration zones associated with Archean lode deposits. *Economic Geology*, **79**, 1131–41.

Mallet JL (1992) Discrete smooth interpolation in geometric modelling. *Computer-aided Design*, **24**, 177–91.

Martel SJ, Pollard DD (1989) Mechanics of slip and fracture along small faults and simple strike-slip-fault zones in granitic rock. *Journal of Geophysical Research-Solid Earth and Planets*, **94**, 9417–28.

Matthäi SK, Fischer G (1994) Quantitative modeling of fault-fluid-discharge and fault-dilation-induced fluid-pressure variations in the seismogenic zone. *Geology*, **24**, 183–6.

Matthäi SK, Garofalo P (1999) Three-dimensional shear zone and joint geometry and permeability in the Sigma Gold Mine, Canada. In: *Mineral Deposits: Processes to Processing* (ed. Stanley CJ), pp. 1411–4. Balkema, Rotterdam.

Matthäi SK, Roberts S (1997) Transient versus continuous fluid flow in seismically active faults: an investigation by electric analogue and numerical modelling. In: *Fluid Flow and Transport in Rocks. Mechanisms and Effects* (eds Jamtveit B, Yardley BWD), pp. 263–95. Chapman & Hall, London.

National Institute of Health USA (1998) *Scion Image for Windows*. http://rsb.info.nih.gov/nih-image/.

Naylor MA, Mandl G, Sijpesteijn CHK (1986) Fault geometry in basement-induced wrench faulting under different initial stress states. *Journal of Structural Geology*, **8**, 737–52.

Nicholson R, Pollard DD (1985) Dilation and linkage of en-echelon cracks. *Journal of Structural Geology*, **7**, 583–90.

Oliver NHS, Bons PD (2001) Mechanisms of fluid flow and fluid–rock interaction in fossil metamorphic hydrothermal systems inferred from vein–wallrock patterns, geometry and microstructure. *Geofluids*, **1**, 137–62.

Petit J-P, Mattauer M (1995) Palaeostress superimposition deduced from mesoscale structures in limestone: the Matelles exposure, Languedoc, France. *Journal of Structural Geology*, **17**, 245–56.

Pollard DD, Segall P (1987) Theoretical displacements and stress near fractures in rock: with applications to faults, joints, veins, dikes, and dissolution surfaces. In: *Fracture Mechanics of Rocks* (ed. Atkinson BK), pp. 277–349. Academic Press–Harcourt Brace Jovanovich Publishers, London.

Ridley JR, Mengler F (2000) Lithological and structural controls on the form and setting of vein stockwork orebodies at the Mount Charlotte gold deposit, Kalgoorlie. *Economic Geologist*, **95**, 85–98.

Robert F (1983) Étude du mode de mise en place des veines aurifère de la mine Sigma, Vald'Or Québec. PhD Thesis. Université de Montréal, Montréal.

Robert F (1989) Internal structure of the Cadillac tectonic zone southwest of Val d'Or, Abitibi greenstone belt, Quebec. *Canadian Journal of Earth Sciences*, **26**, 2661–75.

Robert F (1990) Structural setting and control of gold–quartz veins of the Val d'Or area, southeastern Abitibi Subprovince. In: *Gold and Base Metal Mineralization in the Abitibi Subprovince, Canada, with Emphasis on the Quebec Segment* (eds Ho SE, Robert F, Groves DI), pp. 167–209. Geol. Key Centre and University Extension, Perth.

Robert F (1994) *Vein Fields in Gold District: the Example of Val D'or, Southern Abitibi Subprovince, Quebec*, pp. 295–302. Geological Survey of Canada, Ottawa.

Robert F, Boullier A-M, Firdaous K (1995) Gold–quartz veins in metamorphic terranes and their bearing on the role of fluids in faulting. *Journal of Geophysical Research*, **100**, 12861–12879.

Robert F, Brown AC (1984) Progressive alteration associated with gold–quartz–tourmaline veins at the Sigma mine, Abitibi Greenstone belt, Quebec. *Economic Geology*, **81**, 593–616.

Robert F, Brown AC (1986a) Archean gold-bearing quartz veins at the Sigma mine, Abitibi Greenstone belt: part I. Geological relations and formations of the vein systems. *Economic Geology*, **81**, 578–92.

Robert F, Brown AC (1986b) Archean gold-bearing quartz veins at the Sigma mine, Abitibi Greenstone belt: part II. Vein paragenesis and hydrothermal alteration. *Economic Geology*, **81**, 593–616.

Robert F, Kelly WC (1987) Ore-forming fluids in Archean gold-bearing quartz veins at the Sigma mine, Abitibi Greenstone belt, Quebec, Canada. *Economic Geology*, **82**, 1464–82.

Robert F, Poulsen KH (1997) World-class Archean gold deposits in Canada: an overview. *Australian Journal of Earth Sciences*, **44**, 329–51.

Robin PYF, Cruden AR (1994) Strain and vorticity patterns in ideally ductile transpression zones. *Journal of Structural Geology*, **16**, 447–66.

Segonds D, Mallet JL, Lévy B (1997) Smooth triangulated surfaces: G^1 continuity for ray-tracing. In: *Society of Exploration Geophysicists Annual Meeting, Dallas, USA*.

Sylvester AG (1988) Strike-slip faults. *Geological Society of America Bulletin*, **100**, 1666–703.

Simpson GDH (2000) Synmetamorphic vein spacing distributions: characterisation and origin of a distribution of veins from NW Sardinia, Italy. *Journal of Structural Geology*, **22**, 335–48.

Spooner ETC, Barrie CT (1993) A special issue devoted to Abitibi ore deposits in a modern context — Preface. *Economic Geology*, **88**, 1307–22.

Teyssier C, Tikoff B (1999) Fabric stability in oblique convergence and divergence. *Journal of Structural Geology*, **21**, 969–74.

Tikoff B, Greene D (1997) Stretching lineations in transpressional shear zones: an example from the Sierra Nevada batholith, California. *Journal of Structural Geology*, **19**, 29–39.

Vearncombe JR (1998) Shear zones, fault networks, and Archean gold. *Geology*, **26**, 855–8.

Willemse EJM, Pollard DD, Aydin A (1996) Three-dimensional analyses of slip distributions on normal fault arrays with consequences for fault scaling. *Journal of Structural Geology*, **18**, 295–309.

Wong L, Davis DW, Krogh TE, Robert F (1991) U–Pb zircon and rutile chronology of Archean greenstone formation and gold mineralization in the Val d'Or region, Quebec. *Earth and Planetary Science Letters*, **104**, 325–36.